

## 7. COMPARED CYCLICITY AND DIAGENESIS OF TWO ANOXIC DEPOSITS IN THE CARIBBEAN DOMAIN: THE PLEISTOCENE–HOLOCENE OF CARIACO BASIN (SITE 1002) AND THE UPPER CRETACEOUS LA LUNA–QUERECUAL FORMATION (NORTH VENEZUELA)<sup>1</sup>

Pierre Cotillon,<sup>2</sup> Aurélie Picard,<sup>2</sup> and Nicolas Tribovillard<sup>3</sup>

### ABSTRACT

Two geographically close hemipelagic deposits are compared: (1) the Pleistocene–Holocene part of the Cariaco Basin succession off Venezuela drilled in Hole 1002C and (2) the Upper Cretaceous (Cenomanian to Santonian) La Luna–Querecual Formation, which crops out in northern Venezuela from the Sierra de Perija, west of the Gulf of Maracaibo, to the Gulf of Paria eastward. This analysis is based on thin-section descriptions, porosity data, and examination of core photographs.

Despite their very different ages, these formations are similar in facies, structure, and diagenetic behavior. Their facies are calcareous black shales rich in organic matter and planktonic remains such as foraminifers, radiolarians, and diatoms. Their structures result in a high-frequency cyclic fabric with superimposed units ranging from obliquity cycles to annual varves, as well as several types of solar and pluriannual El Niño–type cycles. In the Cariaco succession, the frequencies of pluriannual cycles have been determined by a statistical study on deposits with standardized compaction and sedimentation rates to convert the thickness of cycles to a scale proportional to their duration. Their diagenetic behavior is signaled by (1) early carbonate precipitation under bacterial control leading to beige micritic layers, (2) carbonate and siliceous concretions before major compaction, (3) recrystallization, (4) deformation from compaction, and (5) dissolution.

The main observed lithologic differences between the Cariaco Basin and the La Luna–Querecual successions result from the weak diagenetic evolution for the Cariaco series. This evolution reached an ultimate state for the La Luna–Querecual Formation because of tectonic overburial, leading to recrystallization and precipitation of large carbonate and siliceous nodules, and to cementation. Thus, it is appropriate to consider the Cariaco series as an illustration of the initial state of the La Luna Formation.

Major common characteristics relative to the genesis of the two deposits signify the similar anoxic depositional environment (900 and 500 m deep for the Cariaco and the La Luna–Querecual Formations, respectively), similar paleogeographic and latitude (2°–15°N) settings on the Guyanese Craton Margin, and similar climate and current controls leading to varves and lower order depositional cycles. Cycles are manifested as an alternation of light layers enriched with planktonic microfossils deposited during dry periods and of dark layers composed of clay–organic complexes with a maximum of detrital quartz, deposited during wet periods.

The major discrepancy in the sedimentation rates (128 m/m.y. for the Cariaco series, 13 m/m.y. for the La Luna Formation) of equally compacted deposits fits principally with different tectonic and sea-level histories in the two series. Indeed, the sedimentary fluxes were low during the Late Cretaceous, before the Laramide orogeny. They were much more important in the Pleistocene–Holocene because of enhanced land erosion due to block faulting in the Venezuelan Andes and the Guyanese Craton and to a lower sea level.

### INTRODUCTION

The four holes at Ocean Drilling Program (ODP) Site 1002 are located in the central part of the Cariaco Basin, at a water depth of 892–893 m (Figs. 1, 2). From these holes was recovered a Quaternary succession containing cycles having various millimeter to decimeter thicknesses and a dominant black color caused by high concentrations of organic matter. A detailed observation of cores has revealed the presence of some lithologic concretions formed by early diagenetic carbonate precipitation.

The Late Cretaceous of northern Venezuela (Fig. 2) includes a black shale formation, which was the primary source rock of hydrocarbons exploited in this country (Tribovillard et al., 1991a, 1991b). This anoxic facies is called the La Luna Formation in western Venezuela and particularly in the Transversale de Barquisimeto (Aubouin, 1975) (Figs. 1, 2) and Querecual in eastern Venezuela (Fig. 2, Ber-

gantin area). It is composed of laminated black sediments enriched with carbonate and siliceous concretions. This facies is included in a transgressive unit of Cenomanian to Senonian age, deposited under a water column <500 m deep (Tribovillard and Stephan, 1989).

These two series are very similar with respect to depositional setting and lithology. We wished, therefore, to begin an investigation to compare microscopic and macroscopic cycles to more precisely determine their periodicities and depositional controls and to ascertain the origin of their diagenetic concretions. In particular, we asked whether the late Quaternary deposits of the Cariaco Basin, for which the environmental interpretation is already well understood (Peterson et al., 1991, Lin et al., 1997), can be considered an analogue for the Cretaceous black shales of northern Venezuela in their initial diagenetic state.

### RECENT QUATERNARY OF THE CARIACO BASIN

The study of Quaternary sediments from the Cariaco Basin is based on the following:

1. Thirty-three thin sections sampled after an induration by araldite infilling from the 19 cores recovered from Hole 1002C, which reached 170.1 meters below seafloor (mbsf). The micro-

<sup>1</sup>Leckie, R.M., Sigurdsson, H., Acton, G.D., and Draper, G. (Eds.), 2000. *Proc. ODP, Sci. Results*, 165: College Station, TX (Ocean Drilling Program).

<sup>2</sup>Université Claude Bernard Lyon 1, UFR des Sciences de la Terre, 29-43 Boulevard du 11 Novembre, 69622 Villeurbanne Cédex, France. Pierre.Cotillon@univ-lyon1.fr

<sup>3</sup>Université des Sciences et Techniques Lille 1, Sédimentologie et Géodynamique, Bât. SN5, 59655 Villeneuve d'Ascq Cédex, France.

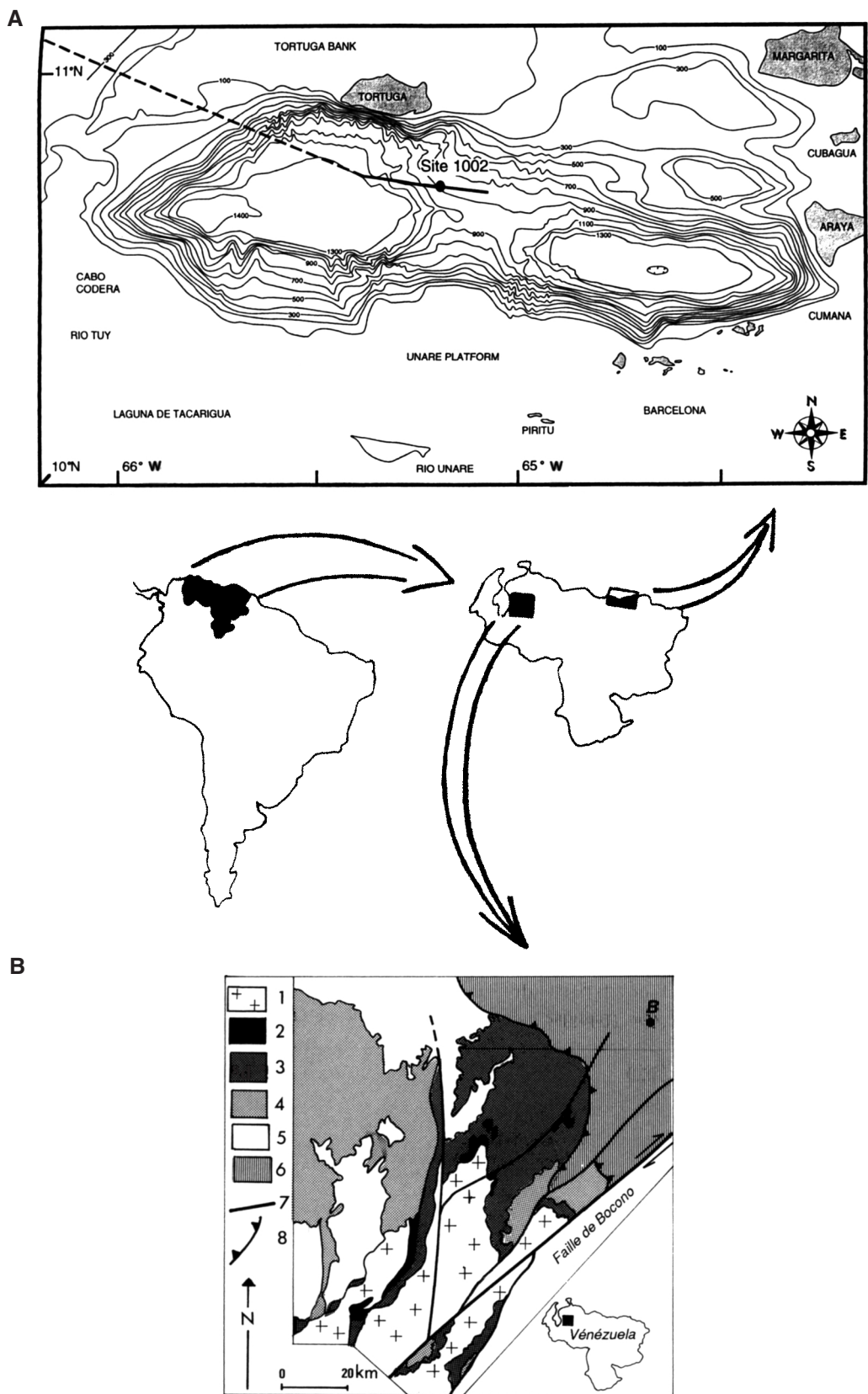


Figure 1. The Venezuelan areas included in this study. **A.** Cariaco Basin with bathymetric curves. Dashed line = trackline of the *JOIDES Resolution*. **B.** The Transversale de Barquisimeto (Aubouin, 1975) shown by a simplified geological map: B = Barquisimeto; 1 = crystalline outcrops, 2 = Jurassic, 3 = Cretaceous, 4 = Cenozoic, 5 = post-thrusting deposits, 6 = allochthonous formations, 7 = major faults, and 8 = thrusts.

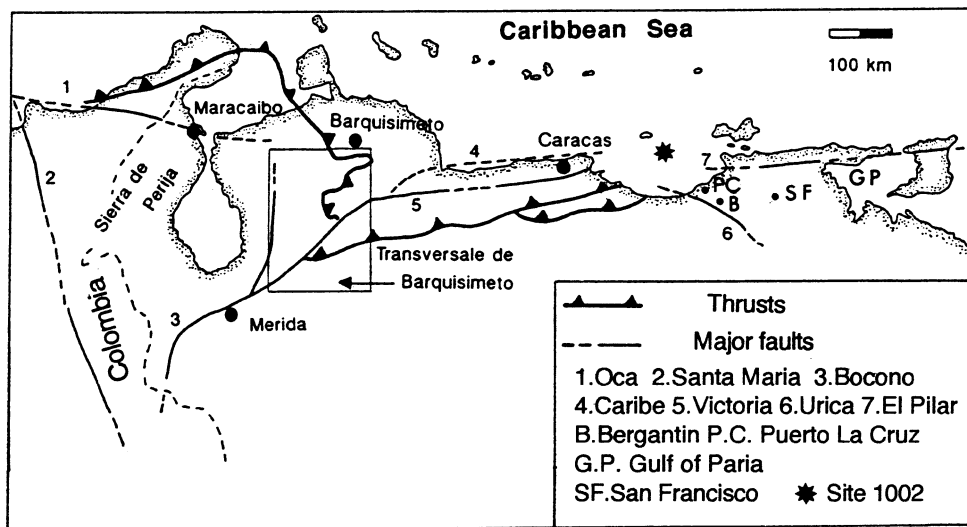


Figure 2. Simplified structural map of northern Venezuela showing the Transversale de Barquisimeto location (after Tribouillard et al., 1991a).

scopic observation of thin sections focused particularly on lithologic structures that define cyclicity.

2. Porosity measurements (142) provided by Larry Peterson that allowed us to take compaction into account.
3. Black-and-white photographs of the 19 cores from Hole 1002C.
4. Previous research on the Cariaco Basin and other studies that ascribe the thinnest lithologic cycles to annual varves (Donegan and Schrader, 1982; Peterson et al., 1991; Thunell et al., 1995; Hughen et al., 1996). Thus, we were able to conduct a statistical study on the duration of cycles other than varves and to reach a conclusion about their probable origin.

## Cyclicity

### Elementary Cycles

Elementary cycles correspond to the thinnest units distinguishable in thin sections. Their thickness varies along the cores, primarily because of compaction; for instance, an average cycle thickness value of 1.25 mm was found in Section 165-1002C-1H-4 (5 mbsf), compared to an average value of 0.65 mm in Section 165-1002C-3H-7 (27 mbsf). In most thin sections, the elementary cycles exhibit a constant structure (Fig. 3): light laminae including pelagic debris derived from planktonic foraminifers, nannoflora, diatoms, and pieces of pelecypod shells; and dark laminae enriched in clay, reduced iron, and brown organic matter. The latter are generally concentrated in tiny, irregular discontinuous and wispy films that may correspond to components of fossil bacterial mats. Such structures off the Peruvian coast have been observed and previously described (Brodie and Kemp, 1994) and in the Santa Monica Basin off California (Hagadorn et al., 1995). In the dark laminae, the fossiliferous content is close to that of the light laminae, although more limited and devoid of diatoms.

In some cycles, the light laminae are thicker (Christensen, 1991); in others, the dark laminae are thicker. Usually, elementary cycles include variable amounts of detrital quartz, phosphate debris, and particularly fish scales, which are usually concentrated in the dark laminae. In the Cariaco Basin, the elementary cycles are regarded as varves (Peterson et al., 1991).

### Lower Order Cycles

Lower order cycles can be observed in thin sections and in core photographs. For example, interval 165-1002C-3H-7, 42–45 cm, dis-

plays 10 major bundles of varves creating alternating light and dark bands, which are composed of from two to 11 varves (Fig. 3). However, most of the cycles are from 3 to 5 yr long, a duration close to the frequency of El Niño cycles. Such cycles have been described in Quaternary deposits of the Santa Monica Basin (Quinn et al., 1987; Christensen et al., 1994; Hagadorn et al., 1995). As many as four orders of cycles may be observed per thin section.

Thicker, multicentimeter cycles may be disclosed in core photographs. Their analysis led to a quantitative study of their duration, which required correction for compaction and sedimentation rate through the drilled series to make cycle thicknesses directly proportional to their length (Fig. 4). Only cycles >5 cm thick have been considered to avoid the effect of bioturbation on the results; indeed, 5 cm is the average thickness of mixed layers in pelagic deposits (e.g., Guinasso and Shink, 1975; Peng et al., 1979; Nittrouer et al., 1984; De Master et al., 1985).

Cycles appear on the photographs as an alternation of light and dark bands corresponding either to a variation in  $\text{CaCO}_3$  content, a variation of the redox potential (Cotillon et al., 1994), or their combined effects (Cotillon, 1991). By convention, the base of a cycle corresponds to the base of a dark layer overlying a light layer (Cotillon, 1991; Sageman et al., 1997). The reworked intervals and turbidites observed in the visual core descriptions (generally appearing as light layers) were not considered in calculating the number of cycles per core. Comparison of the durations of lower order cycles can be done once the compaction and sedimentation rate are standardized through the drilled series. An average porosity was calculated for each core from values measured in each section (Table 1). Because the cementation by precipitation in interstitial voids is nearly absent in the sediment, porosities were regarded as proportional to the compaction (Beaudoin et al., 1984). All the porosities (i.e., compaction intensities) were made equal to that of Core 165-1002C-9H, located in the middle of the cored Cariaco sequence. This implies a correction of core lengths: a shortening above Core 9H and a lengthening below. The result is virtual sediment section S2, 183 m long, divided into 20 "cores," 19 of which are 9.45 m long (average core length for the Hole 1002C succession) (Fig. 4).

The average thickness of varves in each core allows us to calculate an average sedimentation rate. For cores not sampled, or where the varves are obliterated by bioturbation, the sedimentation rate was adjusted to the average sedimentation rate of adjacent cores. A second correction deals with the sedimentation rate of S2, so that the thicknesses of cycles become directly proportional to their duration.

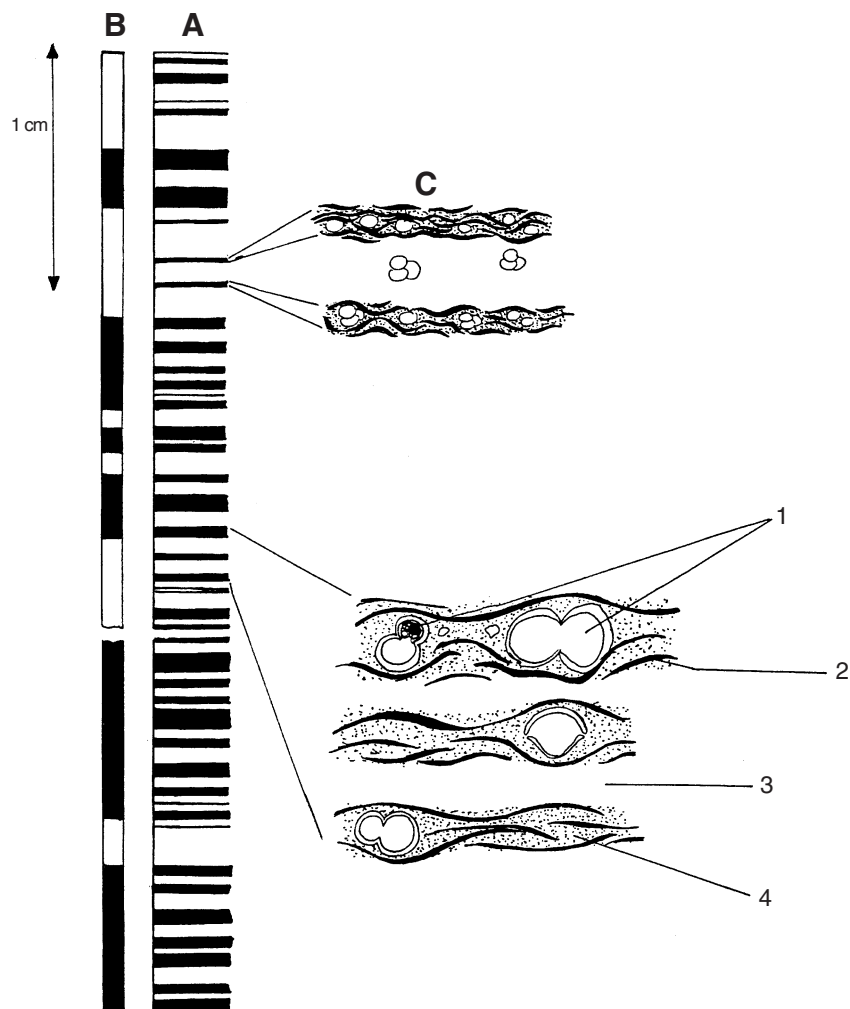


Figure 3. Schematic illustration of two orders of dark and light cycles occurring in a thin section from the Cariaco series (Sample 165-1002C-3H-7, 42–45 cm). **A.** Varved succession. **B.** Grouping of varves in dark/light lower order cycles. **C.** Enlarged varves: (1) foraminifer shells, empty or filled with brown organic matter, (2) wispy film of organic matter in a dark layer, (3) micrite forming a light layer, and (4) clay–organic matter matrix.

This correction makes all sedimentation rates equal to that of Core 165-1002C-3H, where varves are well exposed. This results in a second virtual sediment section (S3), including 21 cores (20 of which have the standard length of 9.45 m) where a duration can be assigned to each cycle (Fig. 4). The average duration of cycles in each of the 21 cores is transferred to a histogram (Fig. 5). These durations vary from 17 to 56 yr (with an average value of 37 yr) and are distributed in three groups:

1. Group A, corresponding to the five upper cores, with 22 yr as the average duration;
2. Group B, with five cores and cycles 48 yr long on average. This group has the lowest concentration of laminated intervals; and
3. Group C, with 11 cores and average cycles of 40 yr (virtual Cores 3S-11 through 3S-21), where laminations are well marked again.

Average durations of 22 and 40 yr for the cycles of Groups A and C are close to solar cycles 22 and 44 yr long (Perry, 1994). A control by solar-activity cycles has been assumed for  $^{14}\text{C}$  production and abundance of *Globigerina bulloides* in the Cariaco Basin (Peterson et al., 1991) with periodicities of 200 and 140 yr and for organic productivity on the northern Gulf Coast (Heydari et al., 1997) with 12- and 24-yr cycles. Hughen et al. (1996) have recognized decade- to century-scale climatic oscillations during the last deglaciation, based on the lami-

nated fabric of Cariaco deposits. Decadal cycles also have been indicated in anoxic laminated deposits of the Santa Monica and Santa Barbara Basins off California (Hagadorn et al., 1995).

Additional lower order megacycles are also apparent in the synthetic Hole 1002C succession (Fig. 6). Thirteen megacycles can be distinguished based on laminated/bioturbated deposits, with a total duration of 580 k.y. (Haug et al., 1998). This gives an average duration equal to 44.6 k.y., close to one of the obliquity periods.

A more detailed analysis is based on the S3 series, where the thicknesses of 12 cycles measured on the lithologic column are directly proportional to their duration. These durations are plotted on a histogram (Fig. 7) where the modal value is located between 20 and 40 k.y. The average duration of the seven cycles included in this value is 38.2 k.y.; that of the two cycles located between 40 and 60 k.y. is 56.6 k.y. These two values are close to those of the obliquity periods (41 and 54 k.y.).

Finally, we have verified that the number of cycles per 100 k.y., calculated for each core and >5 cm thick, is positively correlated with sedimentation rate (Fig. 8). The same correlation was obtained previously from other successions (Cotillon, 1991; P. Cotillon, unpubl. data).

### Light Beige Micritic Inclusions

Discontinuous and slender inclusions of light beige micrite, poor in sulfur, can be observed (Fig. 9). These inclusions appear either as

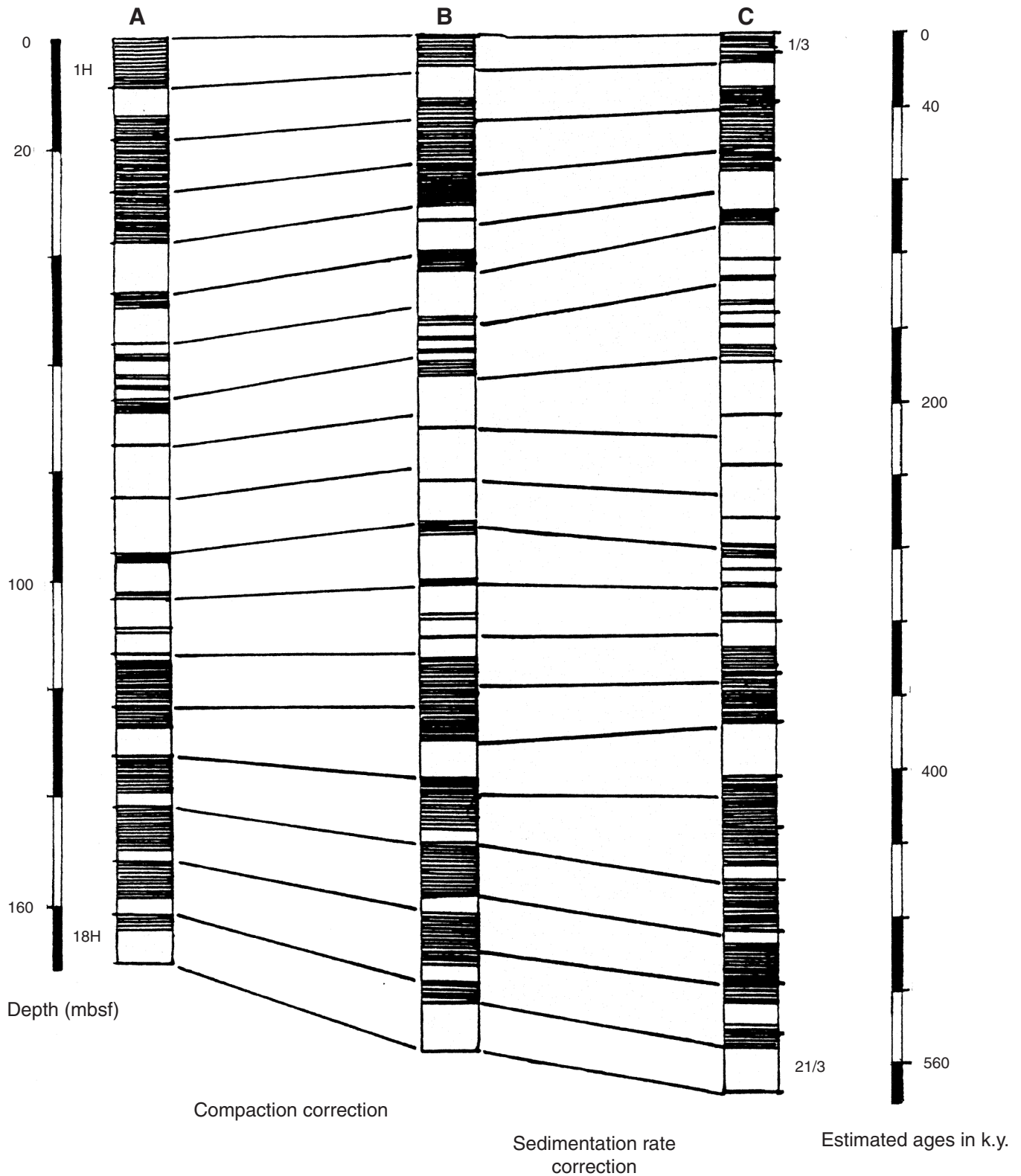


Figure 4. Process for making the compaction and the sedimentation rates uniform through the Hole 1002C succession. **A.** Actual drilled series (S1) with 18 cores (Cores 165-1002C-1H through 18H; average length: 9.45 m). **B.** Transformed series (S2) after a compaction correction, with 20 cores (19 with the standard length of 9.45 m). **C.** Transformed series (S3) with 21 cores (20 with the standard length of 9.45 m) after a sedimentation rate correction.

Table 1. Cariaco Basin, Hole 1002C.

Core, section	Depth (mbsf)	Corrected depth (mbsf)	Dry density (g/cm <sup>3</sup> )	Corrected porosity	Core, section	Depth (mbsf)	Corrected depth (mbsf)	Dry density (g/cm <sup>3</sup> )	Corrected porosity
165-1002C-					10H-1	85.15	85.05	1.174	51.46
1H-1	0.75	0.75	0.454	84.87	10H-2	85.92	85.72	1.097	48.34
1H-2	2.25	2.25	0.685	78.61	10H-3	87.43	87.04	1.030	51.11
1H-3	3.75	3.75	0.497	79.34	10H-4	88.96	88.37	1.213	49.50
1H-4	5.25	5.25	0.658	73.74	10H-5	90.50	89.71	1.182	44.28
1H-5	6.75	6.75	1.007	60.69	10H-6	92.06	91.07	0.976	48.07
1H-6	7.84	7.84	1.293	55.21	10H-7	93.50	92.32	0.910	41.55
2H-1	9.14	9.12	0.881	71.01	10H-8	95.07	93.69	1.159	49.18
2H-2	10.64	10.59	0.853	65.09	11H-2	94.92	94.86	0.875	49.81
2H-3	12.14	12.05	0.893	62.72	11H-3	96.41	96.26	0.686	50.13
2H-4	13.64	13.52	0.899	64.00	11H-4	97.97	97.72	0.991	44.74
2H-5	15.14	14.98	0.899	66.37	11H-5	99.67	99.32	1.419	37.19
2H-6	16.64	16.45	0.891	62.51	11H-6	101.27	100.83	1.494	37.94
2H-7	17.62	17.40	0.884	65.55	11H-7	102.80	102.26	1.140	48.89
3H-1	18.66	18.63	0.913	62.95	11H-CC	104.25	103.63	1.156	46.54
3H-2	20.14	20.05	0.883	65.23	12H-1	104.20	104.08	1.234	42.69
3H-3	21.64	21.49	0.892	65.08	12H-2	105.40	105.10	1.235	41.14
3H-4	23.17	22.96	0.904	70.43	12H-3	106.95	106.42	1.078	35.88
3H-5	24.67	24.40	0.899	64.06	12H-4	108.45	107.70	1.243	43.12
3H-6	26.20	25.87	0.933	61.82	12H-5	109.96	108.98	1.164	42.18
3H-7	27.18	26.81	0.975	61.41	12H-6	111.51	110.31	1.045	43.73
4H-1	28.14	28.12	1.020	59.11	12H-7	113.01	111.59	1.167	46.52
4H-2	29.64	29.68	0.957	59.86	12H-CC	114.49	112.85	1.143	42.99
4H-3	31.17	31.07	1.066	59.87	13H-1	113.64	113.55	1.210	45.78
4H-4	32.74	32.60	0.992	59.04	13H-2	114.73	114.50	1.058	49.52
4H-5	34.32	34.14	0.996	63.50	13H-3	116.43	115.99	0.854	46.91
4H-6	35.88	35.65	1.102	56.91	13H-4	117.73	117.12	0.850	50.85
4H-7	36.82	36.57	1.124	58.33	13H-5	119.23	118.43	0.961	40.79
5H-1	37.65	37.60	0.898	60.68	13H-6	120.73	119.74	1.084	46.25
5H-2	39.15	39.01	0.989	58.80	13H-7	122.23	121.05	0.880	50.86
5H-3	40.65	40.42	1.090	56.69	14H-1	122.75	122.71	1.156	47.08
5H-4	42.22	41.89	0.953	59.46	14H-2	123.71	123.56	1.241	41.26
5H-5	43.72	43.30	0.900	59.33	14H-3	125.22	124.89	1.189	43.74
5H-6	45.22	44.71	1.034	59.41	14H-4	126.73	126.23	1.253	40.45
5H-7	46.72	46.12	0.866	62.92	14H-5	128.30	127.61	1.367	36.80
6H-2	47.41	47.31	1.156	55.04	14H-6	129.89	129.02	1.271	40.20
6H-3	48.90	48.66	1.119	57.54	15H-1	132.37	132.31	1.254	47.95
6H-4	50.39	50.01	1.089	55.96	15H-2	133.31	133.13	1.224	37.15
6H-5	51.90	51.37	1.163	58.72	15H-3	134.84	134.46	1.071	38.22
6H-6	53.45	52.77	1.103	53.92	15H-4	136.31	135.73	1.092	41.33
6H-7	55.05	54.22	1.114	46.84	15H-5	137.81	137.04	1.162	43.22
6H-8	56.55	55.57	1.216	49.04	15H-6	139.34	138.37	1.240	35.17
7H-1	56.64	56.53	1.148	63.04	15H-7	140.72	139.57	0.983	40.33
7H-2	57.62	57.28	1.010	46.97	15H-8	142.22	140.87	0.971	43.91
7H-3	69.07	58.60	1.096	48.46	16H-1	141.80	141.75	1.123	50.04
7H-4	60.52	59.84	1.144	50.28	16H-2	142.36	142.24	1.153	42.28
8H-5	62.09	61.17	1.023	46.67	16H-3	143.93	143.62	1.029	45.31
7H-6	63.64	62.49	1.059	48.65	16H-4	145.69	145.16	1.089	45.43
7H-7	65.24	63.86	1.019	47.89	16H-5	147.21	146.50	1.128	46.15
7H-8	66.73	65.13	1.136	48.71	16H-6	148.71	147.81	1.137	43.24
8H-1	65.87	65.81	0.930	52.72	16H-7	150.26	149.17	1.047	44.54
8H-2	66.69	66.52	1.016	54.05	16H-8	151.71	150.44	0.956	47.01
8H-3	68.17	67.81	1.102	51.94	17H-1	151.63	151.61	1.214	41.13
8H-4	69.69	69.14	0.945	52.48	17H-2	153.21	153.13	1.432	34.23
8H-5	71.19	70.44	0.983	54.19	17H-3	154.77	154.64	1.393	31.81
8H-6	72.72	71.77	1.153	46.48	17H-4	156.35	156.17	1.366	36.16
8H-7	74.24	73.10	1.073	44.18	17H-5	157.90	157.67	1.218	42.28
8H-8	75.72	74.39	1.037	51.09	17H-6	159.40	159.12	1.221	41.07
9H-1	76.67	75.64	0.750	56.94	17H-7	160.38	160.07	1.281	43.34
9H-2	76.85	76.78	1.055	59.07	18H-1	161.13	161.10	1.283	38.45
9H-3	78.35	78.23	0.983	59.90	18H-2	162.63	162.54	1.234	40.63
9H-4	79.91	79.74	1.079	50.08	18H-3	164.13	163.97	1.336	37.16
9H-5	81.35	81.13	1.065	53.84	18H-5	166.11	165.87	1.073	38.25
9H-6	82.85	82.58	1.163	53.84	18H-6	167.56	167.26	1.244	36.50
9H-7	84.28	83.96	1.203	43.05	18H-7	169.11	168.74	1.256	38.21

irregular, aligned, and discontinuous laminae (from 1 to 10 mm long and 0.1 mm wide) or as isolated and rounded heaps, with maximum dimensions of 0.05–0.12 mm. These micritic patches may include organic remains such as foraminifers; their precipitation and induration are precocious because they precede compaction and were recovered as early as the uppermost core. The patches can result from precipitation controlled by anaerobic bacterial activity; this precipitation, however, is not a syndimentary process because it also occurs in bioturbated sections of the Cariaco succession related to aerobic episodes.

### Diagenetic Processes

Diagenetic processes were first indicated during shipboard core descriptions as dolomitic concretions forming either indurated layers

a few centimeters thick or isolated nodules at 28, 60, 65, 80, 123, and 170 mbsf. The deepest layer, which also marks where the coring at Site 1002 was stopped, is partly silicified. Dolomite commonly appears during the bacterial decay of methane in anoxic environments (von Rad et al., 1995; Vasconcelos and McKenzie, 1997). Methane is actually present in cores of the Cariaco series, leading to many degassing structures.

Calcitic concretions are also present as sparitic round or ovoid inclusions, the latter lengthened parallel to the stratification; 0.2–0.6 mm is their largest dimension. They are generally polycrystalline, with radial calcite crystals (Fig. 10). Some of them result from the crystallization of a micritic filling of foraminifers. These concretions are observed beginning in Section 165-1002C-5H-6 (45.5 m depth), but they become larger and more numerous with greater depth and are present down to the base of Hole 1002C. The shells of foraminifers

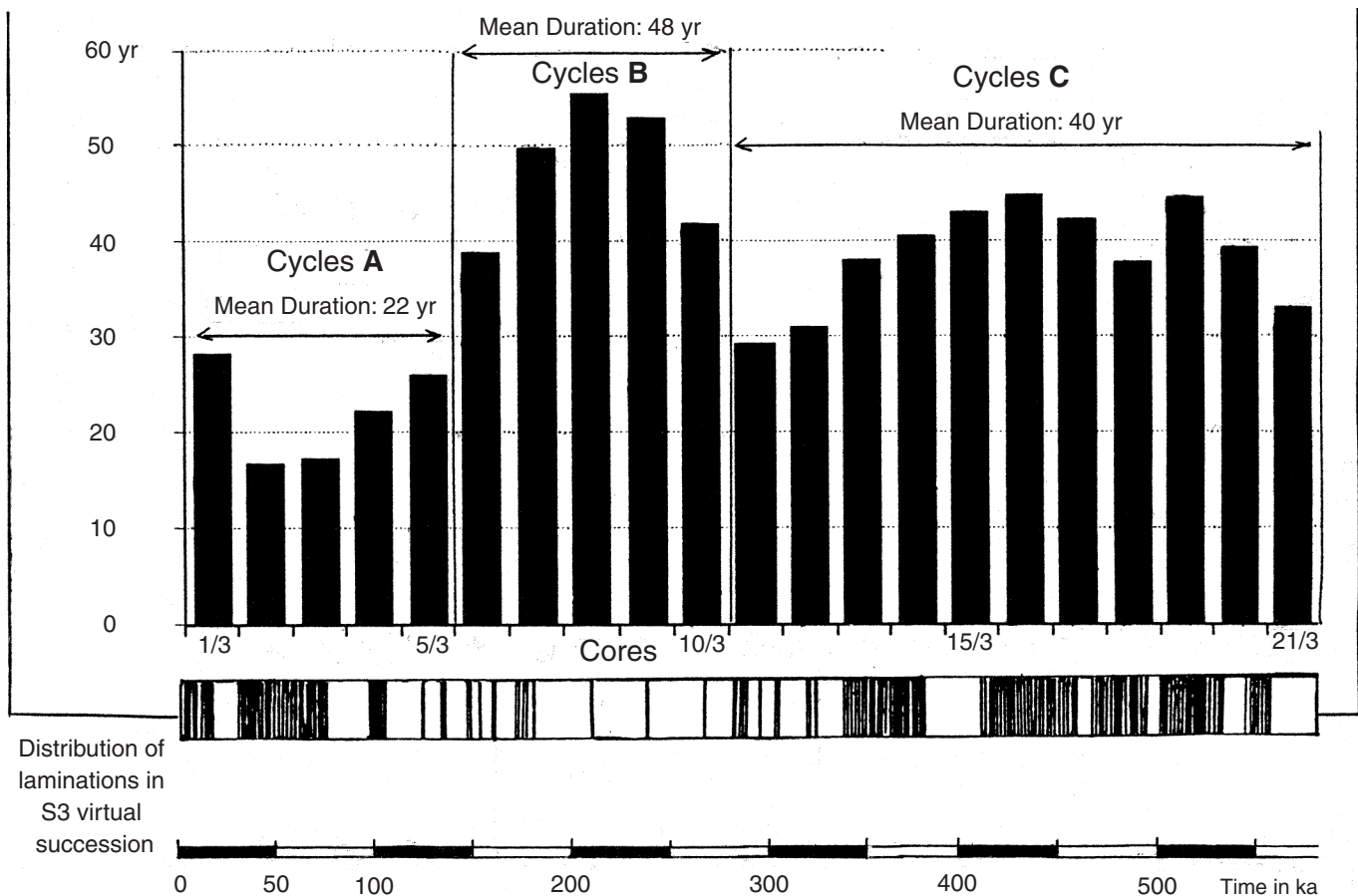


Figure 5. Average duration of dark and light lower order cycles in each core of the virtual series S3. Three groupings of durations are apparent.

fers in places are filled with pyrite as early as the uppermost core, but most remain empty or partly filled with sediment down to the base of drilling.

### UPPER CRETACEOUS OF THE LA LUNA-QUERECUAL FORMATION

On both sides of the transcurrent Bocono Fault (Fig. 11), the La Luna Formation is characterized by marly anoxic facies, including varied amounts of carbonate and siliceous concretions. Most Venezuelan oil is derived from this formation.

North of the fault, there are outcrops of alternating marls and marly limestones that are 200 m thick, black, laminated, and rich in such organic matter and phosphatic debris as fish scales. Here the formation is Cenomanian to Santonian in age and is subdivided into three members (Fig. 11).

South of the fault, the La Luna Formation is only 60 m thick and is Coniacian-Santonian in age. It is composed of a monotonous succession of indurated, micaceous, and laminated marls, overlying an eroded surface. Its richness in organic matter (as much as 6% of the sediment) and fish scales is conspicuous. The same facies continues eastward in the Querecual Formation, which thickens up to 740 m.

As for the Pleistocene-Holocene sediments of the Cariaco Basin, the analysis of the La Luna-Querecual Formation is based on observation of thin sections from cores drilled from the La Luna Formation as well as from the Querecual Formation (near Puerto La Cruz, Bergantín, and San Francisco [Fig. 2]), which is the eastern equivalent of the La Luna. Several orders of cycles have been identified and described as well as various types of organic remains and diagenetic

processes. In this study, porosity measurements made by the Paris School of Mines Laboratory have been considered.

### Primary Structures

#### Cyclicity

Cyclicity is expressed again through elementary and lower order cycles of various thicknesses. Elementary cycles are best expressed in the darkest intervals, where fine and discontinuous light layers are included. The dark layers, formed of a clay-organic matter complex, may be nearly black; they are discontinuous and deformed against organic remains such as planktonic foraminifers and radiolarians and also against detrital quartz (Fig. 12). The light layers, generally discontinuous, are calcareous and formed of planktonic remains (mainly foraminifers and coccoliths).

The thickness of elementary cycles varies from 0.01 to 0.08 mm. Given the hypothesis that elementary cycles are varves, the average varve thickness over the total thickness of the La Luna Formation (200 m), implies that ~16 m.y. of time are represented by this unit, compared to 15.4 m.y. for the biostratigraphic time scale (Gradstein et al., 1994). The assumption of elementary cycles as varves therefore seems reasonable to a first approximation.

Lower order cycles are made of (1) a dark bundle of elementary cycles resulting from a clayey-organic matrix and always relatively enriched in detritic quartz; and (2) a light bundle, generally less thick and sometimes recrystallized with calcite (Fig. 12).

The number of elementary cycles in these units is so variable that the corresponding durations vary from several years to several tens of years. Also, light bundles always include fewer varves than dark bundles. Note that counting elementary cycles is difficult because of their

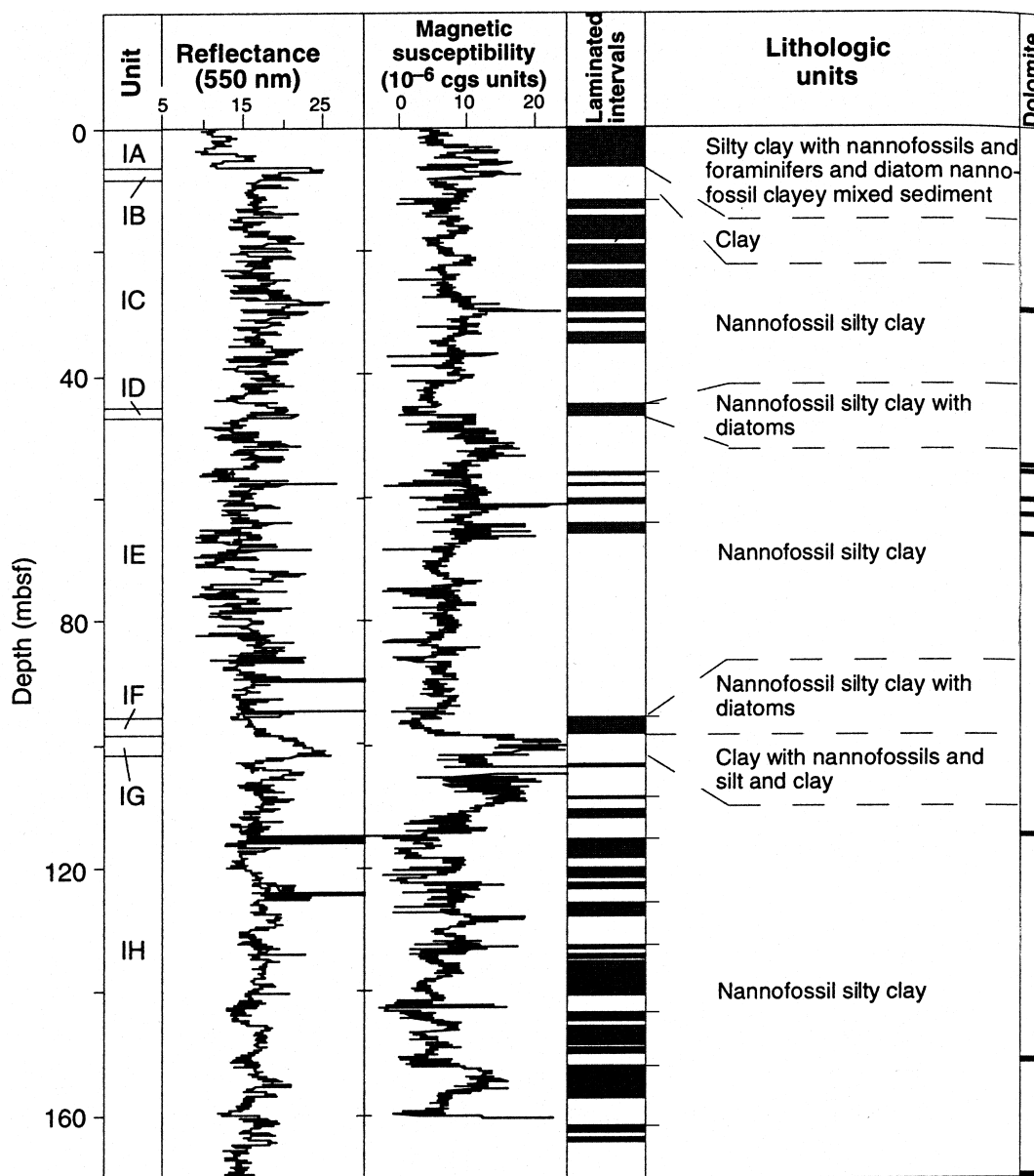


Figure 6. Low-frequency cycles forming the Cariaco succession in Hole 1002C (after Sigurdsson, Leckie, Acton, et al., 1997). IA: Bioturbated deposits (silty clay with nannofossils, foraminifers, and diatoms). IB: Clear greenish to yellowish brown clay. IC: Olive-gray to light olive gray clayey bioturbated deposits with nannofossils. ID: Olive-gray clayey bioturbated deposit with nannofossils and diatoms. IE: Greenish gray to dark greenish gray clayey bioturbated deposit with nannofossils. IF: Dark olive green clayey bioturbated deposit with nannofossils and diatoms. IG: Light bluish gray to pale brown clay with nannofossils and silts. IH: Olive-green to olive-gray clayey bioturbated deposit with nannofossils. Limits of the 13 megacycles are marked on the right edge of the laminated intervals column.

thinness and because of deformation resulting from compaction. Nevertheless, among 25 thin sections including laminations, five exhibit one lower order cycle with 10–12 varves, two show one cycle with 22–28 varves, one contains cycles with 22–24 varves, and two display cycles with an average of six varves.

Field sections of the La Luna–Querecual Formation illustrate the occurrence of larger cycles, denoting an orbital control of sedimentation. For instance, north of the Bocono Fault, outcrops of the lower La Aguada Member exhibit an alternation of dark gray, laminated limestones and shales, with limestone beds 20–60 cm thick and thinner shale layers (Tribovillard et al., 1991b). Assuming an average thickness of nearly 50 cm for the corresponding cycles, and given the mean sedimentation rate of the La Luna Formation (200 m/15.4 m.y. = 13 m/m.y.), a duration close to 38 k.y. is obtained for these cycles.

This is in the range of the 39-k.y. period of one of the obliquity cycles at 72 Ma (Berger et al., 1989).

#### Beige Micritic Layers

Beige micritic layers are 0.05 to 0.25 mm thick on average, always irregular, and rarely continuous. The latter behavior is represented by ovoid, tapered heaps, parallel to stratification, with rare organic inclusions such as foraminifers (Fig. 13). Beige micritic layers or heaps are sometimes superimposed and joined together, but usually they are isolated and sparse. They may correspond to precipitates linked to bacterial activity. The division of primarily continuous or semicontinuous layers into ovoid units may result from compaction, which also generates deformation and moves disrupted units. Similar

structures have been depicted in the Lower Cretaceous of Deep Sea Drilling Project Site 535 in the Gulf of Mexico (Cotillon and Rio, 1984).

### Biological Content

Sections of the La Luna–Querecual Formation, characterized by abundant carbonate and siliceous concretions (Fig. 14), generally include many ammonite and inoceramid shells. In thin section, debris from inoceramid shells, foraminifers (Hedbergellidae and Heterohelicidae), and calcitized radiolarians, but no diatoms, is observed. Planktonic foraminifers are always bigger and more numerous in the light layers of lower order cycles, where their chambers are filled with calcite, than in the dark layers.

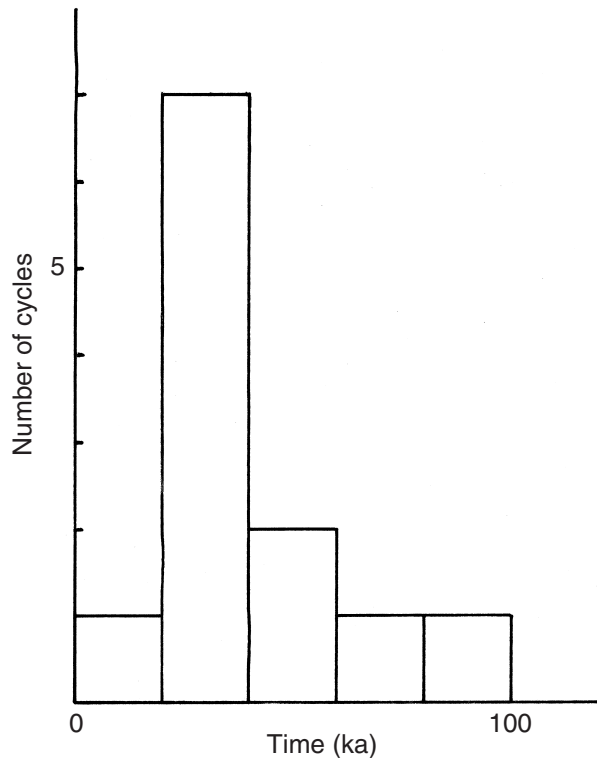


Figure 7. Distribution of durations for the 12 dark/light megacycles comprising the virtual series S3 (see Fig. 4).

### Diagenetic Evidence

Indications of compaction are frequent and varied, including crushing of biogenic structures like foraminifer shells (Fig. 15), deformation of the laminae of elementary cycles against radiolarians or foraminifers (Fig. 16), and pressure-dissolution features such as stylolites and compaction splits.

Planktonic foraminifers have generally lost their shells by dissolution. Only their calcitized molds remain, although these can also be affected by dissolution—all the more marked when they are located in dark layers rich in organic matter. The decay of this material, accompanied by a release of  $\text{CO}_2$ , could explain the dissolution features. Two facts may be connected: the occurrence of siliceous concretions and the lack of diatoms.

Carbonate or siliceous concretions as long as 25 mm are abundant in thin sections; they can be several meters in length in field sections. These concretions testify to diagenetic precipitation leading to the genesis of a plentiful cement. This abundance is suggested by weak porosity of the sediment (only 0.25%–4.80% in five samples), proving an important burial partly of tectonic origin (overthrusting). By comparison, sediment nearly as old (middle Campanian), drilled at Site 1001 and buried under 480 m of younger formations, exhibits a porosity of nearly 24% (Fig. 17). Concretions occur early, before a major part of compaction (Tribovillard et al., 1991a). Proof is given by the above-mentioned concretions, reaching a length of 25 mm in thin section (Fig. 18). The matrix of the concretions is recrystallized sparite tending to unify the facies; in the latter, the clay-organic matrix is relegated to dark pelletic heaps. Nevertheless, remains of light-laminae-bearing planktonic debris can be recognized; they become more tightened at one extremity of the nodule. The tightness intensity allows us in this case to define a relative compaction of ~9.

Calcitic recrystallization has occurred in some structures as the filling of foraminiferal chambers. The latter occurred early because it resisted crushing by compaction. Carbonate precipitates other than calcite are rare; some dolomite occurs as sparse rhombohedral crystals. Siliceous layers are also rarely observed. Recrystallization can also affect the light layers of varves that grow thicker and display blurred boundaries. From this state, more pronounced epigenesis can affect the sediment.

### COMPARISON OF THE CARIACO AND LA LUNA–QUERECUAL SUCCESSIONS

The lithology and structure of these deposits show some similarities: dominant marls, dark color, wealth of organic matter, abundance of planktonic remains such as foraminifers, and occurrence of first-

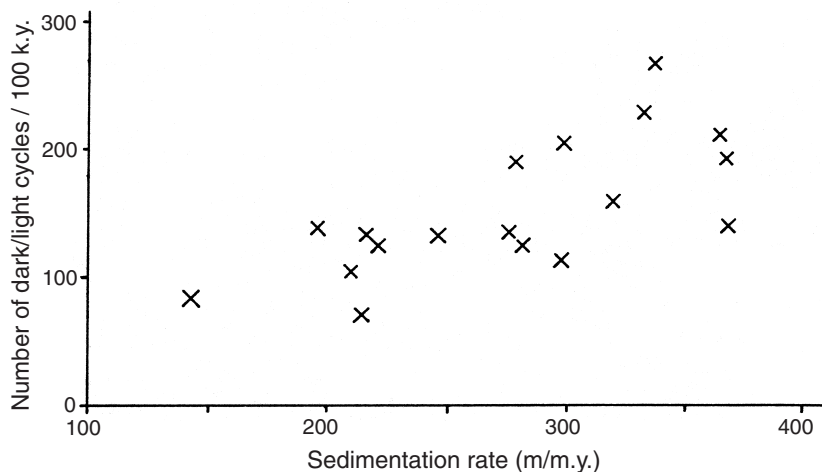
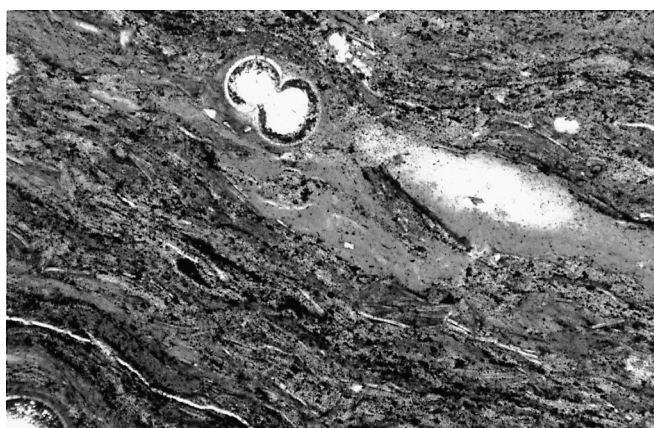


Figure 8. Correlation between the sedimentation rate and the number of dark and light alternating cycles per 100 k.y. for the Cariaco succession ( $r = 0.481$ ). The data points refer to 18 of the 21 cores of the virtual series, S3.



0.2 mm

Figure 9. Light beige micritic inclusions observed in a thin section from the Cariaco succession (Sample 165-1002C-16H-5, 110–113 cm). One inclusion is partially recrystallized. Magnification: 61×.

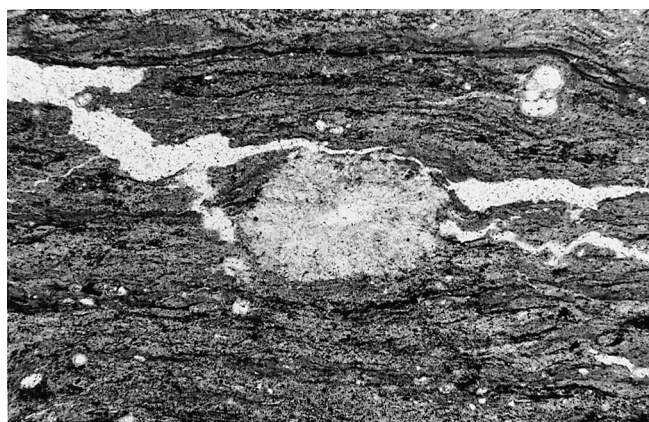
order cycles creating two types of alternation: marl/limestone for the La Luna–Querecual Formation and bioturbated/laminated layers for the Cariaco succession. The difference in importance of diagenetic precipitation (concretions up to several meters in size in La Luna–Querecual and millimeter-scale in the Cariaco succession) is not significant given the disparity of the two diagenetic states.

From a microfacies point of view, the two successions exhibit a laminated structure with elementary cycles formed from two layers: a light one, enriched with materials derived from surface production (planktonic foraminifers, radiolarians, and diatoms, the latter occurring only in the Cariaco deposits); and a dark one, where clay, detrital quartz, and organic matter are concentrated. In the two successions, these fundamental cycles can be regarded as varves; their genesis has been well documented in the Cariaco Basin (Peterson et al., 1991; Huguen et al., 1996). They testify to the seasonal extreme of a tropical climate with a dry season leading to upwelling conditions and high surface productivity and a wet season with increased fluvial runoff.

We used the average thickness of varves to compare the mean sedimentation rates of the La Luna Formation and the Cariaco succession. This required us to make the two deposits equally compacted and then correct them for approximately the same porosity. The chosen porosity (24%) is that of the middle Campanian at Site 1001 (southeastern edge of the Nicaraguan Rise), buried under 500 m of younger deposits (Fig. 17). This value is assumed to illustrate (1) the porosity of the Cariaco succession submitted to the same burial and (2) the porosity of the La Luna–Querecual Formation before its cementation resulting principally from a tectonic burial.

After this correction, the calculated sedimentation rates reached 13 m/m.y. for the La Luna Formation and 128 m/m.y. for the Cariaco succession. This great difference must certainly result from both surface productivity and terrigenous flux. The latter, however, could play a prominent part, given all the nutrients brought by terrestrial runoff (Haq, 1993).

The fabric of the lower order cycles (groupings of light and dark bundles) signifies the same alternation of high-productivity and high-terrigenous inputs as for elementary cycles, with a particularly important concentration of detrital quartz in the dark layers. These cycles are proxies for climatic variations affecting atmospheric and oceanic circulation. The most frequent periodicities registered in the Cariaco Basin (3–5, 20, and 40 yr), possibly related to El Niño and some solar cycles, are not so well recorded and sometimes less clearly expressed



0.3 mm

Figure 10. Rounded sparitic concretion observed in a thin section from Sample 165-1002C-12H-1, 23–26 cm (Cariaco succession). The varval laminae are slightly deformed around the concretion. Magnification: 38×.

in the La Luna–Querecual Formation because of the slower sedimentation rate as well as the diagenetic transformations associated with tectonic activity.

A common occurrence in the two deposits is beige micritic ovoid patches, which may have formed from more or less continuous laminae precipitated under a bacterial control. The patches were lithified before the major compaction, and their early diagenetic formation is demonstrated by a first occurrence at 6.5 m below the top of the uppermost core from Hole 1002C.

Regarding diagenetic processes, abundant criteria reveal that the succession in the Cariaco Basin illustrates the initial state of the La Luna and Querecual Formations. This initial state is a clay and carbonate varved deposit, rich in calcareous and siliceous planktonic remains and in organic matter (the abundance of organic matter and preservation of varves indicate an anoxic environment). Between 0.10 and 1.00 m beneath the sediment/water interface, an oxidation of methane controlled by bacterial activity may be assumed (Raiswell, 1987) as well as carbonate precipitation in an environment becoming more and more alkaline.

Dissolution of calcareous planktonic remains during the decay of organic matter in the upper part of the Cariaco succession could yield part of the carbonate involved in the different types of precipitates: dolomitic layers and concretions from a depth of at least 28.0 m, discontinuous beige micritic layers from at least 6.5 m, and sparitic concretions most often initiated by foraminifer shells from at least 45.0 m. Calcareous infillings of foraminifers, which occur systematically in the La Luna–Querecual Formation, require at Cariaco a burial exceeding the 169-m depth reached in Hole 1002C.

All these precipitates occur before the major compaction. This is demonstrated especially in the La Luna–Querecual Formation by foraminifers devoid of calcite filling and crushed (Fig. 15), whereas the carbonate concretions have preserved the initial thickness of laminations (Fig. 18). Such occurrences are also present in the Cariaco succession. The richness in  $H_2S$  yielded by sulfate reduction may explain the abundance of tiny pyrite grains occurring from the uppermost core of Hole 1002C and filling partly or totally organic voids like foraminifer shells.

It is not easy to verify if sparitic concretions can constitute an initial process leading to the meter-scale carbonate concretions present in the La Luna–Querecual Formation and individualized before the major compaction. Berner (1968) suggested that calcareous nodules, when rapidly formed, could originate from “adipocires”: organic

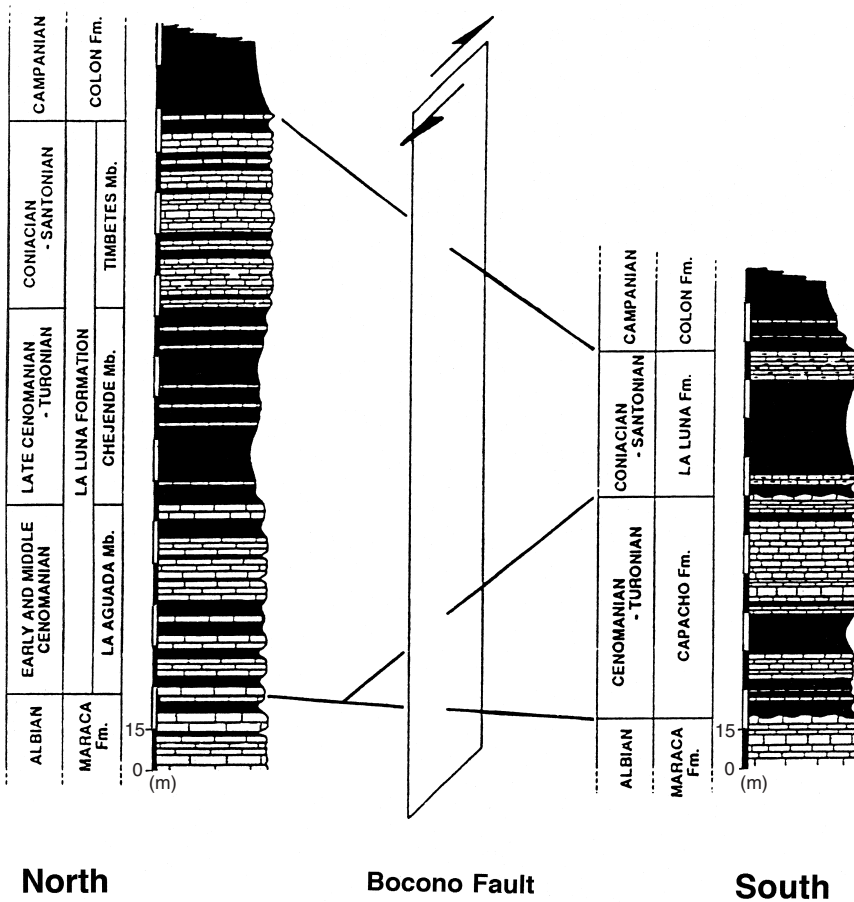


Figure 11. Stratigraphic columns of the La Luna Formation on both sides of the Bocono Fault (after Tribouillard et al., 1991a).

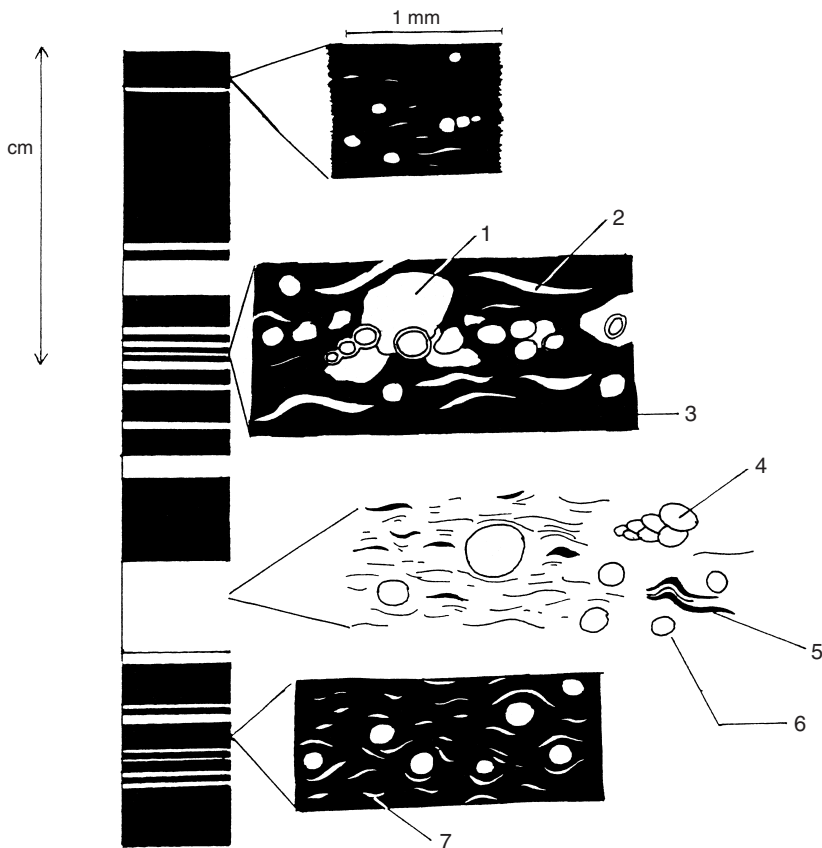


Figure 12. Schematic diagram of lamina bundles with their enlargements as appearing in thin sections from the Querecual Formation (Bergantin, Hole P3-6, 97–100 cm): (1) recrystallized calcite, (2) calcareous layer, (3) clay-organic matrix, (4) recrystallized foraminifer (Heterohelicidae), (5) clay-organic layer interpreted as a relict of a varval dark lamina, (6) calcitized radiolarians, and (7) calcareous layer interpreted as a relict of a varval light lamina.

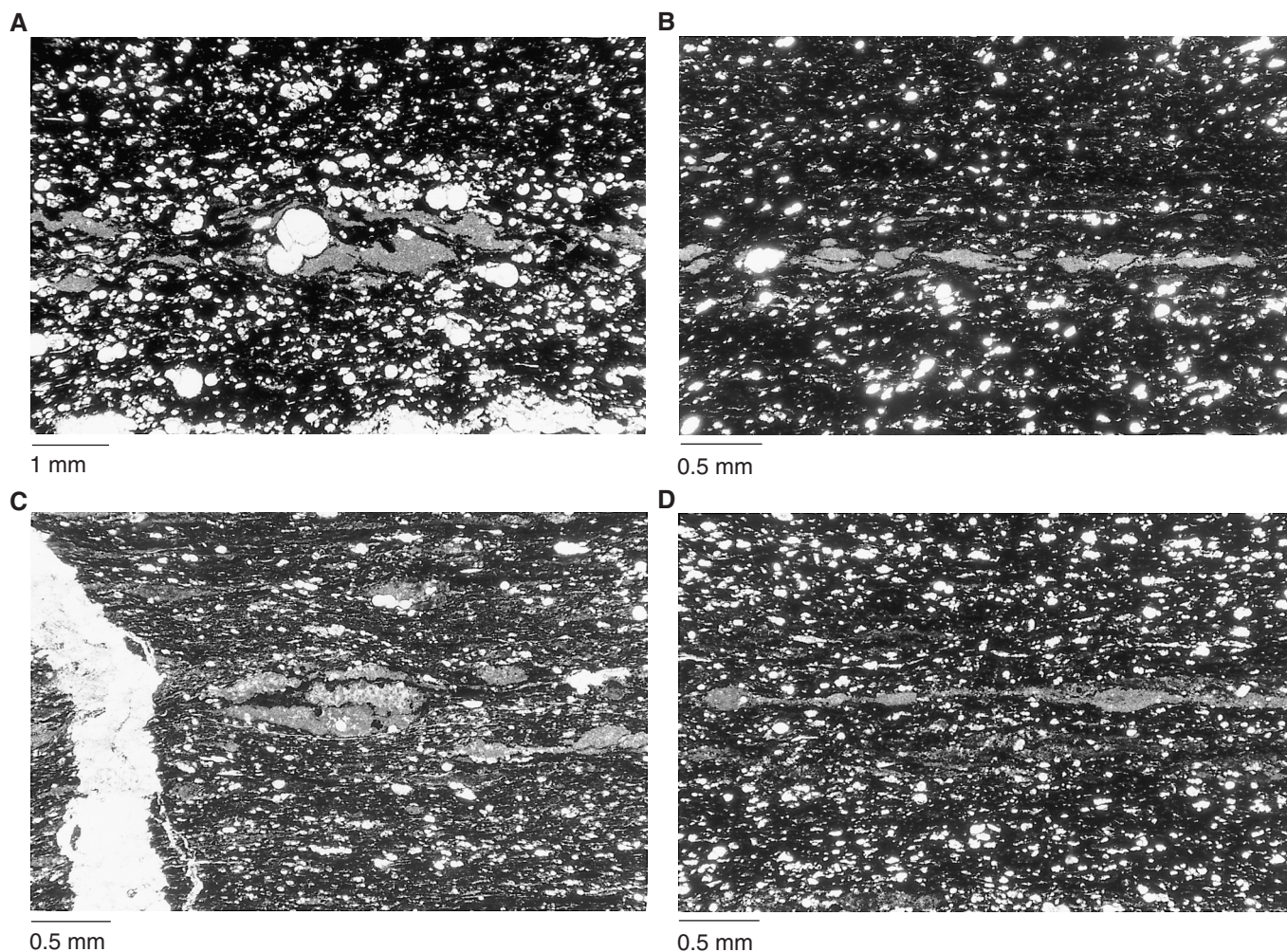


Figure 13. Discontinuous and irregular beige micritic layers (BML) in thin sections from the Querecual Formation showing large quantities of recrystallized planktonic foraminifers. **A.** Deformation of BML around a calcitized foraminifer (magnification: 13×) (Bergantin, Hole 3-2, 187–190 cm). **B.** Aligned BML(s) (magnification: 27×) (Carretera a Turimiquire, Hole 1-2, 130–133 cm). **C.** Deformation of laminae around associated BML(s) (magnification: 27×) (Carretera a Turimiquire, Hole 1-1, 64–67 cm). **D.** Semicontinuous embossed BML(s) assumed to represent the first step of isolated BML individualization (magnification: 27×) (Carretera a Turimiquire, Hole 1-1, 64–67 cm).

products generated by the decay of lipids and proteins of animal origin (e.g., fish and jellyfish). The weak representation obtained by drilling does not permit a choice of either hypothesis.

The abundance of diatoms in the Cariaco series may explain the near absence of siliceous concretions. The only concretion that includes some proportion of silica is that marking the bottom of drilling in Hole 1002C at 167 mbsf. Conversely, the La Luna–Querecual Formation is relatively rich in cherty concretions, but diatoms are absent. This suggests that diatoms and radiolarians probably yielded the major part of the silica that formed some concretions in the La Luna–Querecual Formation. In addition, the siliceous concretions precipitated after the carbonate concretions against which they are deformed (Fig. 19). The recrystallization features occur mostly in the La Luna–Querecual Formation.

### Cycles

Despite important disparities in age, sedimentation rate, and depth of burial, the Upper Cretaceous La Luna–Querecual Formation and the Pleistocene–Holocene succession in the Cariaco Basin share a basic structure as revealed by annual cycles of deposits. The interpreta-

tion of these cycles, demonstrated as a result of upwelling in the Cariaco Basin, can be applied to the La Luna–Querecual Formation despite a major difference in sediment flux. Also, upwelling conditions have been deduced from a geochemical study of the La Luna Formation (Mongenot et al., 1996).

The grouping of varves in bundles, defining lower order subdecadal to decadal cycles, exhibits two sets of cyclic units:

1. Short period units: 3–5 yr for the Cariaco Basin, 6 yr for the La Luna–Querecual Formation. They possibly correspond to the sedimentary record of El Niño cycles. The most ancient proper El Niño events registered up to the present, however, are 5.5 m.y. old (Ortlieb and Macharé, 1993).
2. Solar cycle units, for which some prevailing durations are in evidence: 20–40 yr for the Cariaco succession, 10–12 and 22–24 yr for the La Luna–Querecual Formation.

These lower order cycles are themselves grouped into megacycles well represented in the La Luna–Querecual Formation. The more frequent groupings include five to seven units corresponding to the following brackets: 50–70 to 60–84 yr (for units provided with 10–12

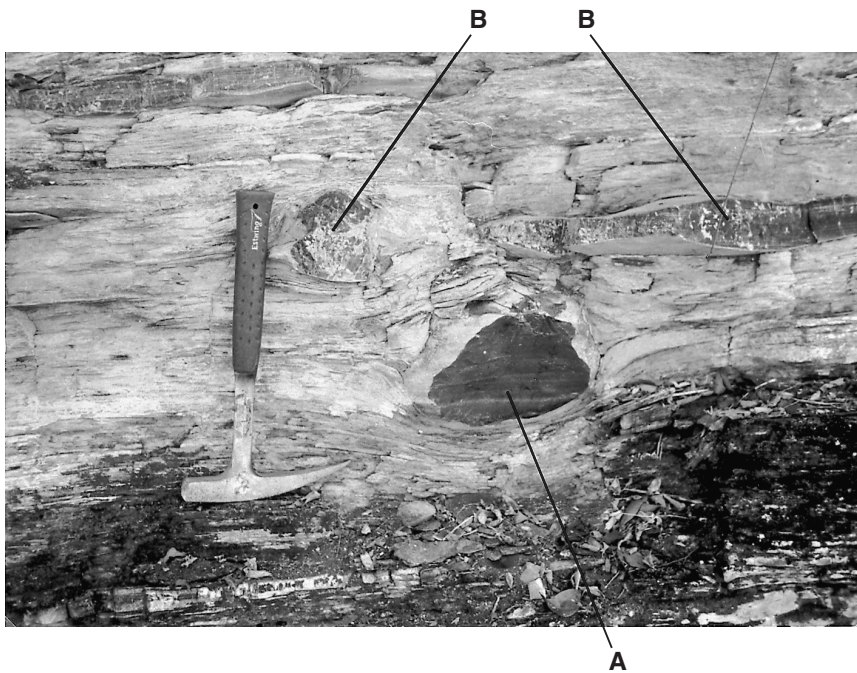
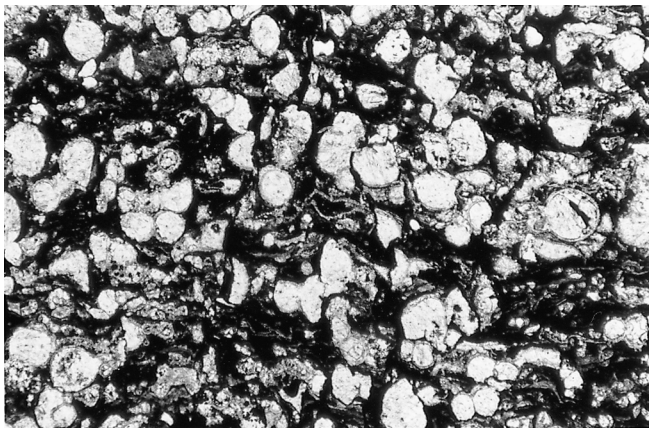


Figure 14. (A) Carbonate and (B) siliceous concretions in an outcrop of the La Luna Formation, near La Haguada. These concretions precipitated before the major compaction.

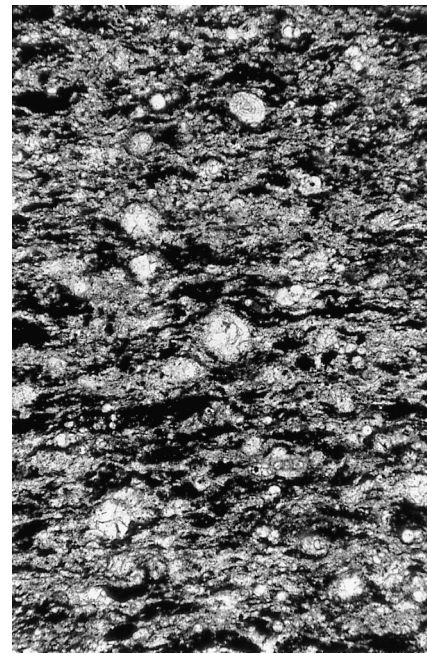


0.2 mm

Figure 15. Biogenic remains as proxies for the compaction in the Querecual Formation: foraminifers filled with calcite are undeformed, whereas shells that remained unfilled are crushed (magnification: 61 $\times$ ) (Guanta, Hole P2-4, 2–5 cm).

varves each); 110–154 to 120–168 yr (for units gathering 22–24 varves). Two values are in evidence: 84 and 168 yr, close to the longest cycles of solar activity.

Finally, obliquity cycles seem have been recorded in the two successions. In the Cariaco series, they correspond to the alternation between predominantly bioturbated and predominantly laminated sections, driven seemingly by the alternation between glacial and nonglacial periods corresponding to periods of higher and lower sea-surface productivity in open basins (e.g., Bowles and Fleischer, 1985; Mortyn and Thunell, 1997; Abrantes et al. 1998). This is not necessarily coincident with the same  $\text{CaCO}_3$  percentage fluctuation, given the possible dissolution or dilution factors. In the Cariaco Basin, isolated from the open Caribbean Sea during glacial times, a reverse correlation between Quaternary climatic periods and productivity is assumed (Peterson et al., 1991). Therefore, laminated intervals of deposits have



0.2 mm

Figure 16. Light laminae of elementary cycles are deformed against calcitized fillings of foraminifer and radiolarian shells in the Querecual Formation, as proof of calcite precipitation in biologic voids before compaction (magnification: 61 $\times$ ) (Guanta, Hole P2-14, 79–82 cm).

recorded the highest productivity. In the La Luna–Querecual Formation, the basic alternation between marls and limestones, or between marls and calcareous marls, seems also to be a result of an orbital control. This pattern has been recognized in all the Mesozoic successions, where it illustrates an alternation of higher (limestones) and lower (marls) sea-surface productivity (Fischer et al., 1985; Herbert and

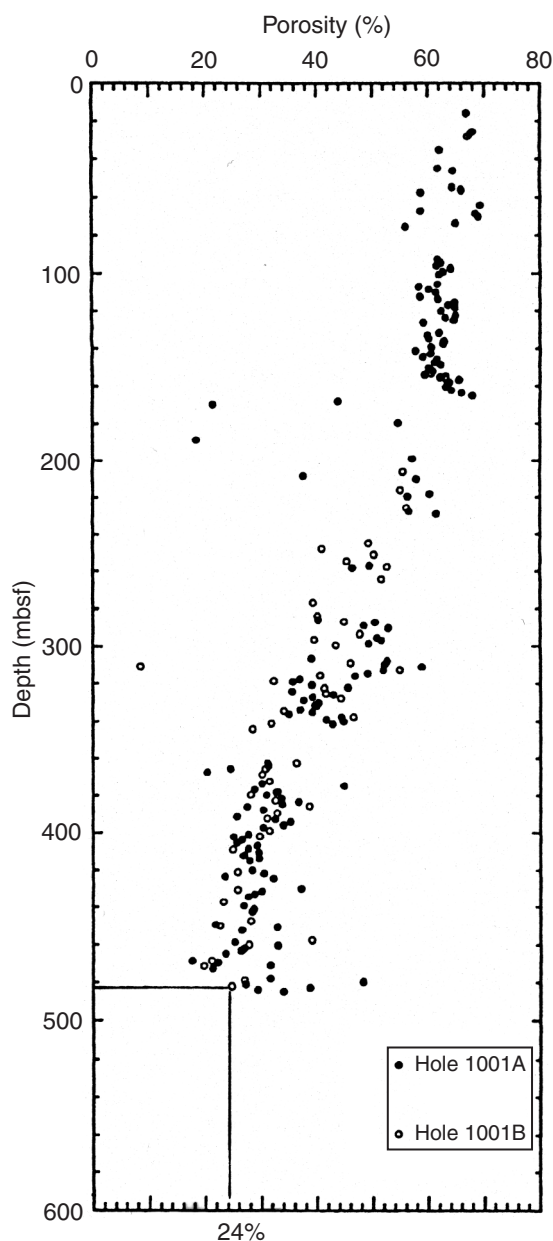
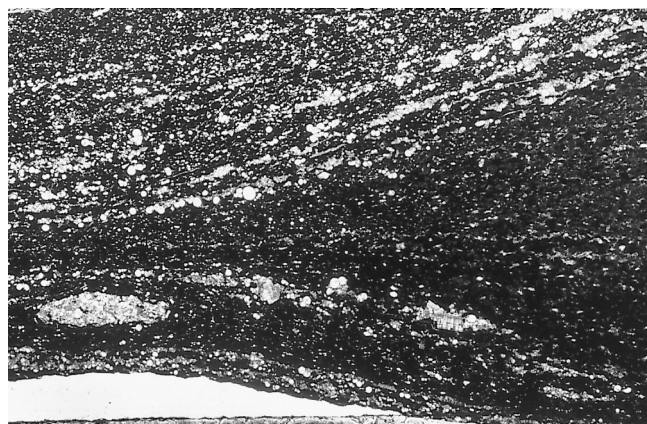


Figure 17. Average porosity (24%) of the middle Campanian at Site 1001 (Sigurdsson, Leckie, Acton, et al., 1997) assumed to illustrate the burial porosity of the La Luna Formation before its tectonic overburden.

Fischer, 1986; Bottjer et al., 1986; Cotillon, 1991; Huang et al., 1993; Cotillon et al., 1994; Erba and Premoli Silva, 1994; Bellanca et al., 1996; Sageman et al., 1997) if the dilution feature is not considered. Consequently, a first attempt at correlation leads us to draw parallels between the carbonate beds of the La Luna–Querecual Formation and laminated intervals in the Cariaco series.

The striking similarities in the two series—in facies, structures, and depositional environments—despite very different ages (as much as 90 m.y.) can be justified by (1) a permanence of paleogeographic and latitudinal setting lying in a marginal position on the northern edge of the South America Craton, between 2°N and 15°N latitude; and (2) common seasonal climatic controls characterized by an alternation of wet and dry conditions leading to seasonal atmospheric and marine currents. Thus, Marcellari and De Vries (1987) have demon-



1 mm

Figure 18. Carbonate concretion, 25 mm long, in a sample from the Querecual Formation, examined in thin section. The precocity of carbonate precipitation is proved by the fossilization of an early and wide spacing of fine carbonate laminae in the center of the concretion (magnification: 15X) (Bergantin, Hole P3-2, 3–6 cm).

strated the occurrence of upwelling and anoxia in northwestern South America during the Late Cretaceous. Both events characterize a local prolonged occurrence of the Cenomanian–Turonian Oceanic Anoxic Event (Arthur et al., 1987). Beyond these regional factors, a permanence of El Niño events in the Pacific as well as rhythms of solar activity variations must be envisaged.

## CONCLUSIONS

The upper Pleistocene–Holocene of the Cariaco Basin and the Upper Cretaceous of the La Luna–Querecual Formation are marine hemipelagic deposits that accumulated under a water column several hundred meters deep. However, the latter formation includes large mollusk shells and seems to reflect closer coastal environments. These two deposits are very similar with respect to their facies, which are principally clays and marls; and to their general fabric, in which appears a fundamental cyclic pattern, particularly in its finest fabric (i.e., annual varves). These varves consist of a light layer having a planktonic character, with concentrations of foraminifers and diatoms; and a dark layer where organic and terrigenous products prevail; each couplet resulting from a seasonal sedimentation that can be observed at present in the Cariaco Basin, in the Santa Barbara Basin, and in the Gulf of California. The fundamental cyclicality of these deposits is in fact recording an alternation of dry seasons, with upwelling dynamics resulting in a spike of planktonic production; and wet seasons, with strong fluvial inputs.

Varves are grouped in bundles that may be recording subdecadal to decadal periodicities, such as those of the El Niño system and of solar activity. The longest cycles visible in the two formations approximately correspond in period with the obliquity periodicity. Lithologically, they appear as a decimetric marl/limestone alternation in the La Luna–Querecual outcrops and as successions of bioturbated and laminated intervals in cored series of the Cariaco Basin. This recurrence during the Pleistocene–Holocene of Upper Cretaceous structures linked to global and regional climatic forcing must be brought closer to a permanence of paleogeographic setting.

Particular structures testify to carbonate precipitation of bacterial origin, manifested as beige micritic patches that are either irregular, discontinuous, and deformed layers or ovoid heaps. A suite of early diagenetic processes are recorded in the Cariaco Basin because of the

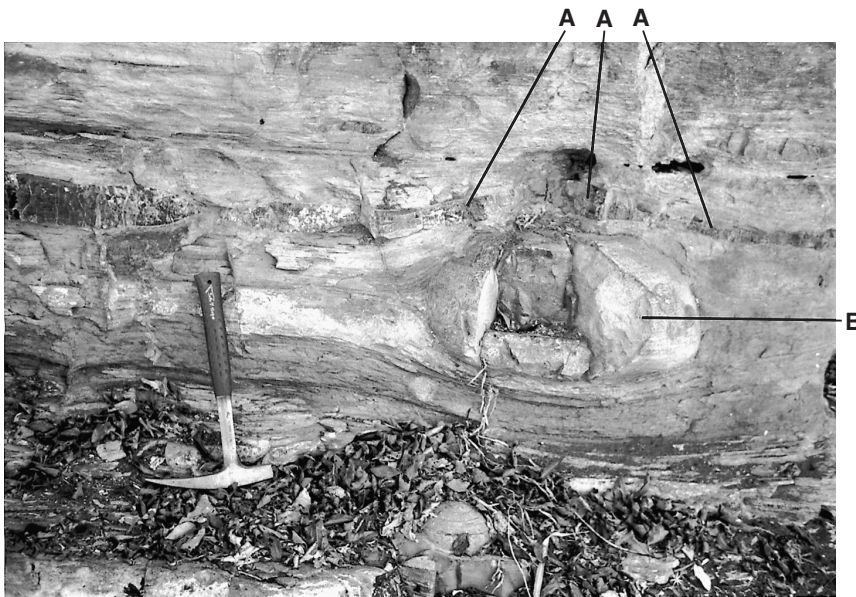


Figure 19. (A) Siliceous and (B) carbonate concretions in an outcrop of the La Luna Formation near Cheyende. The siliceous concretion has precipitated last and is deformed against the carbonate concretion.

shallow depth of the burial of drilled sediments. These processes are compaction, genesis of concretions, and recrystallization.

Compaction allows us to observe the chronology of some processes like the precipitation of carbonate and the formation of siliceous concretions. Genesis of concretions is always early and before the major part of compaction. Precipitation of these concretions resulted from solutions enriched in dissolved products: (1) carbonate derived from biogenic and inorganic structures during periods of CO<sub>2</sub> enrichment caused by bacterial decay of organic matter and (2) silica derived from diatoms and radiolarians.

Field or core observations of the La Luna–Querecual Formation reveal that the carbonate concretions precipitated before the siliceous ones. Comparison of diagenetic processes between the two successions, despite their very different stages of progress, allows us to conclude that the Cariaco succession is a good analogue of the initial state of the La Luna–Querecual Formation.

Finally, the sole significant discrepancy between the two series is that the rate of sedimentation is 10–30 and 3–8 times slower for the La Luna and the Querecual successions, respectively. This disparity may be attributed to very different terrigenous, then biogenic, flux intensities (the latter having induced a great divergence in planktonic production). In short, this discrepancy reflects two epochs of sedimentation: (1) for the La Luna–Querecual Formation, a quiet tectonic episode preceding the Laramide orogenesis and characterized by low topography (Mongenet et al., 1996) and a high sea level leading to a sequestration of detrital materials in coastal and estuarine environments; and (2) for the Cariaco succession, a sequence deposited during the Pliocene–Pleistocene, characterized by lower sea level and block faulting that affected the Venezuelan Andes and the Guyanese Craton and led to a rejuvenation of relief and to enhanced erosion.

#### ACKNOWLEDGMENTS

We thank Larry Peterson for his assistance with porosity data through Hole1002C and the revised biostratigraphy of the succession of Cariaco Basin, Bernard Beaudoin and Martine Audignier of the Paris School of Mines for their porosity data from some samples of the La Luna Formation, Maurice Renard for providing all facilities for the sampling of the Querecual core sections, Angeline Miller of the ODP for many thorough corrections of form and language, and

Mark Leckie and Walter Dean for helpful review of the manuscript. Financial support for analysis was provided by ODP France.

#### REFERENCES

- Abrantes, F., Baas, J., Hafliason, H., Rasmussen, T., Klitgaard, D., Loncaric, N., and Gaspar, L., 1998. Sediment fluxes along the northeastern European Margin: inferring hydrological changes between 20 and 8 kyr. *Mar. Geol.*, 152:7–23.
- Arthur, M.A., Schlanger, S.O., and Jenkyns, H.C., 1987. The Cenomanian–Turonian oceanic anoxic event, II. Palaeoceanographic controls on organic-matter production and preservation. In Brooks, J., and Fleet, A.J. (Eds.), *Marine Petroleum Source Rocks*. Geol. Soc. Spec. Publ. London, 26:401–420.
- Aubouin, J., 1975. Réflexion sur les bordures pacifiques, l'exemple des cordillères américaines. *C. R. Acad. Sci. Ser. 2*, 280D:2633–2636.
- Beaudoin, B., Cojan, I., Fries, G., and Pinoteau, B., 1984. Lois de décompaction et approche des évolutions du taux de sédimentation dans les forages pétroliers du Sud-Est de la France. *Doc. BRGM*, 95-11:133–148.
- Bellanca, A., Claps, M., Erba, E., Masetti, D., Neri, R., Premoli Silva, I., and Venezia, F., 1996. Orbitally induced limestone/marlstone rhythms in the Albian–Cenomanian Cison section (Venetian region, Northern Italy): sedimentology, calcareous and siliceous plankton distribution, elemental and isotope geochemistry. *Palaeogeogr., Palaeoclimatol., Palaeoecol.*, 126:227–260.
- Berger, A., Loutre, M.F., and Dehant, V., 1989. Influence of the changing lunar orbit on the astronomical frequencies of the Pre-Quaternary insolation patterns. *Paleoceanography*, 4:555–564.
- Berner, R.A., 1968. Calcium carbonate concretions formed by the decomposition of organic matter. *Science*, 159:195–197.
- Bottjer, D.J., Arthur, M.A., Dean, W.E., Hattion, D.E., and Savrda, C.E., 1986. Rhythmic bedding produced in Cretaceous pelagic carbonate environments: sensitive recorders of climatic cycles. *Paleoceanography*, 1:467–481.
- Bowles, F.E., and Fleischer, P., 1985. Orinocco and Amazon river sediment input to the Eastern Caribbean basin. *Mar. Geol.*, 68:53–72.
- Brodie, I., and Kemp, A.E.S., 1994. Variation in biogenic and detrital fluxes and formation of laminae in late Quaternary sediments from the Peruvian coastal upwelling zone. *Mar. Geol.*, 116:385–398.
- Christensen, C.J., 1991. An analysis of sedimentation rates and cyclicity in the laminated sediments of Santa Monica Basin, California Continental Borderland [M.S. thesis]. Univ. Southern California, Los Angeles.
- Christensen, C.J., Gorsline, D.S., Hammond, D.E., and Lund, S.P., 1994. Non-annual laminations and expansion of anoxic basin-floor conditions in Santa Monica Basin, California Borderland, over the past four centuries. *Mar. Geol.*, 116:399–418.

- Cotillon, P., 1991. Recherche d'un enregistrement de l'eustatisme au large des marges téthysiennes: nouvelle approche par l'étude des variations des flux de matière. Application à la série Tithonique supérieur-Aptien inférieur du site 534 DSDP (Atlantique Central). *Geol. Alp., Mem.*, 18:117–136.
- Cotillon, P., and Rio, M., 1984. Cyclic sedimentation in the Cretaceous of Deep Sea Drilling Project Sites 535 and 540 (Gulf of Mexico), 534 (Central Atlantic) and in the Vocontian Basin (France). In Buffler, R.T., Schlager, W., et al., *Init. Repts. DSDP, 77*: Washington (U.S. Govt. Printing Office), 339–376.
- Cotillon, P., Rousselle, B., Courtinat, B., and Crumiere, J.P., 1994. Evolution of sediment fluxes from the Middle Miocene to Present at ODP site 817 (Townsville Basin, North-eastern Australia) as a record of regional paleogeographic events. *Mar. Geol.*, 121:265–291.
- DeMaster, D.J., McKee, B.A., Nittrouer, C.A., Brewster, D.C., and Biscaye, P.E., 1985. Rates of sediment reworking at the HEBBLE Site based on measurements of Th-234, Cs-137 and Pb-210. *Mar. Geol.*, 66:133–48.
- Donegan, D., and Schrader, H., 1982. Biogenic and abiogenic components of laminated hemipelagic sediments in the central Gulf of California. *Mar. Geol.*, 48:215–237.
- Erba, E., and Premoli-Silva, I., 1994. Orbitally driven cycles in trace-fossil distribution from the Piobiccio core (Late Albian, Central Italy). *Spec. Publ. Int. Assoc. Sedimentol.*, 19:211–225.
- Fischer, A.G., Herbert, T., and Premoli-Silva, I., 1985. Carbonate bedding cycles in Cretaceous pelagic and hemipelagic sediments. In Pratt, L.M., Kauffman, E.G., and Zelt, F.B. (Eds.), *Fine-grained Deposits and Biofacies of the Cretaceous Western Interior Seaway: Evidence of Cyclic Sedimentary Processes*. SEPM Guidebook, 9:1–10.
- Gradstein, F.M., Agterberg, F.P., Ogg, J.G., Hardenbol, J., van Veen, P., Thirry, J., and Huang, Z., 1994. A Mesozoic time scale. *J. Geophys. Res.*, 99:24051–24074.
- Guinasso, N.L., Jr., and Schink, D.R., 1975. Quantitative estimates of biological mixing rates in abyssal sediments. *J. Geophys. Res.*, 80:3032–3043.
- Hagadorn, J.W., Stott, L.D., Sinha, A., and Rincon, M., 1995. Geochemical and sedimentologic variations in inter-annually laminated sediments from Santa Monica Basin. *Mar. Geol.*, 125:111–131.
- Haq, B.U., 1993. Deep-sea response to eustatic change and significance of gas-hydrates for continental margin stratigraphy. *Spec. Publ. Int. Assoc. Sedimentol.*, 18:93–106.
- Haug, G.H., Pedersen, T.F., Sigman, D.M., Calvert, S.E., Nielsen, B., and Peterson, L.C., 1998. Glacial/interglacial variations in production and nitrogen fixation in the Cariaco Basin during the last 580 kyr. *Paleoceanography*, 13:427–432.
- Herbert, T.D., and Fischer, A.G., 1986. Milankovitch climatic origin of mid-Cretaceous black shale rhythms in central Italy. *Nature*, 321:739–743.
- Heydari, E., Wade, W.J., and Anderson, L.C., 1997. Depositional environments, organic carbon accumulation, and solar-forcing cyclicity in Smackover Formation lime mudstones, Northern Gulf Coast. *AAPG Bull.*, 81:760–774.
- Huang, Z., Ogg, J.G., and Gradstein, F.M., 1993. A quantitative study of Lower Cretaceous cyclic sequences from the Atlantic Ocean and the Vocontian Basin (SE France). *Paleoceanography*, 8:275–291.
- Hughen, K., Overpeck, J.T., Peterson, L.C., and Trumbore, S.E., 1996. Rapid climate changes in the tropical Atlantic region during the last deglaciation. *Nature*, 380:51–54.
- Lin, H.-L., Peterson, L.C., Overpeck, J.T., Trumbore, S.E., and Murray, D.W., 1997. Late Quaternary climate change from  $\delta^{18}\text{O}$  records of multiple species of planktonic foraminifera: high-resolution records from the anoxic Cariaco Basin (Venezuela). *Paleoceanography*, 12:415–427.
- Marcellari, C.E., and De Vries, T.J., 1987. Late Cretaceous upwelling and anoxic sedimentation in Northwestern South America. *Palaeogeogr., Palaeoclimatol., Palaeoecol.*, 59:279–292.
- Mongenot, T., Tribovillard, N.P., Desprairies, A., Lallier-Verges, E., and Laggoun-Defarge, F., 1996. Trace elements as palaeoenvironmental markers in strongly mature hydrocarbon source rocks: the Cretaceous La Luna Formation of Venezuela. *Sediment. Geol.*, 103:23–38.
- Mortyn, P.G., and Thunell, R.C., 1997. Biogenic sedimentation and surface productivity changes in the Southern California Borderlands during the last glacial-interglacial cycle. *Mar. Geol.*, 138:171–192.
- Nittrouer, C.A., DeMaster, D.J., McKee, B.A., Cuthall, N.H., and Larsen, I.L., 1984. The effect of sediment mixing on Pb-210 accumulation rates for the Washington Continental shelf. *Mar. Geol.*, 54:201–222.
- Ortlieb, L., and Macharé, J., 1993. Former El Niño events: record from western South America. *Global Planet. Change*, 7:181–202.
- Peng, T.-H., Broecker, W.S., and Berger, W.H., 1979. Rates of benthic mixing in deep-sea sediments as determined by radioactive tracers. *Quat. Res.*, 11:141–149.
- Perry, C.A., 1994. Comparison of solar luminosity model with paleoclimatic data. *Inst. Quat. Stud., TER-QUA Symp. Ser.*, 2:25–37.
- Peterson, L.C., Overpeck, J.T., Kipp, N.G., and Imbrie, J., 1991. A high-resolution late Quaternary upwelling record from the anoxic Cariaco Basin, Venezuela. *Paleoceanography*, 6:99–119.
- Quinn, W.H., Neal, V.T., and Antunez de Mayolo, S.E., 1987. El Niño occurrences over the past four and a half centuries. *J. Geophys. Res.*, 92:14449–14461.
- Raiswell, R., 1987. Non-steady state microbiological diagenesis and the origin of concretions and nodular limestones. In Marshall, J.D. (Ed.), *Diagenesis of Sedimentary Sequences*. Geol. Soc. Spec. Publ. London, 36:41–54.
- Sageman, B.B., Rich, J., Arthur, M.A., Birchfield, G.E., and Dean, W.E., 1997. Evidence for Milankovitch periodicities in Cenomanian-Turonian lithologic and geochemical cycles, Western Interior USA. *J. Sediment. Res.*, 67:286–302.
- Sigurdsson, H., Leckie, R.M., Acton, G.D., et al., 1997. *Proc. ODP, Init. Repts.*, 165: College Station, TX (Ocean Drilling Program).
- Thunell, R.C., Tappa, E., and Anderson, D.M., 1995. Sediment fluxes and varve formation in Santa Barbara Basin, offshore California. *Geology*, 23:1083–1086.
- Tribovillard, N.P., Cotillon, P., Jautée, E., and Stephan, J.F., 1991a. Les nodules carbonatés des formations riches en matière organique du Crétacé supérieur des plates formes vénézuéliennes. *Bull. Soc. Geol. Fr.*, 162:854–866.
- Tribovillard, N.P., Jautée, E., Stephan, J.F., Cotillon, P., Reyre, Y., and Manivit, H., 1991b. Preliminary results of the study of Cretaceous Black Shales of Venezuelan Andes. Paleoenvironmental interpretations. *Palaeogeogr., Palaeoclimatol., Palaeoecol.*, 81:313–321.
- Tribovillard, N.P., and Stephan, J.F., 1989. Surmaturation des Black-shales crétacés des Andes de Mérida (Vénézuëla): rôles respectifs de l'enfouissement sédimentaire et des charriages d'âge éocène. *C. R. Acad. Sci. Ser. 2*, 309:2085–2091.
- Vasconcelos, C., and McKenzie, J.A., 1997. Microbial mediation of modern dolomite precipitation and diagenesis under anoxic conditions (Lagoa Vermelha, Rio de Janeiro, Brazil). *J. Sediment. Res.*, 67:378–390.
- von Rad, U., Schultz, H., and SONNE 90 Scientific Party, 1995. Sampling the Oxygen minimum zone of Pakistan: glacial-interglacial variations of anoxia and productivity (preliminary results, SONNE 90 Cruise). *Mar. Geol.*, 125:7–19.

**Date of initial receipt: 25 May 1998**

**Date of acceptance: 17 June 1999**

**Ms 165SR-011**